International Institute for
Applied Systems Analysis
Schlossplatz 1
A-2361 Laxenburg, Austria

Tel: +43 2236 807 342
Fax: +43 2236 71313
E-mail: publications@iiasa.ac.at
Web: www.iiasa.ac.at

Interim Report IR-09-080

The risk of competitive exclusion during evolutionary branching: Effects of resource variability, correlation and autocorrelation

Jacob Johansson (johans@iiasa.ac.at)
Jörgen Ripa (jorgen.ripa@teorekol.lu.se)
Nina Kuckländer (nina.kucklander@ecologic.eu)

Approved by

Ulf Dieckmann
Leader, Evolution and Ecology Program

June 2010

Contents

Manuscript intended as an article in Theoretical Population Biology:

The risk of competitive exclusion during evolutionary branching: effects of resource variability, correlation and autocorrelation

Jacob Johansson[1,2], Jörgen Ripa[1] and Nina Kuckländer[3]

1. Department of Theoretical Ecology, Ecology building, Lund University, SE-22362 Sweden

2. International Institute of Applied Systems Analysis (IIASA)
Schlossplatz 1, A-2361 Laxenburg, Austria

3. Ecologic Institute, Pfalzburger Str. 43/44, D-10717 Berlin, Germany

Email to corresponding author: johans@iiasa.ac.at

The work was mainly carried out in Department of Theoretical Ecology (1).

ABSTRACT

Evolutionary branching has been suggested as a mechanism to explain ecological speciation processes. Recent studies indicate however that demographic stochasticity and environmental fluctuations may prevent branching through stochastic competitive exclusion. Here we extend previous theory in several ways; we use a more mechanistic ecological model, we incorporate environmental fluctuations in a more realistic way and we include environmental autocorrelation in the analysis. We present a single, comprehensible analytical result which summarizes most effects of environmental fluctuations on evolutionary branching driven by resource competition. Corroborating earlier findings, we show that branching may be delayed or impeded if the underlying resources have uncorrelated or negatively correlated responses to environmental fluctuations. There is also a strong impeding effect of positive environmental autocorrelation, which can be related to results from recent experiments on adaptive radiation in bacterial microcosms. In addition, we find that environmental fluctuations can lead to cycles of repeated branching and extinction.

Keywords: evolutionary branching; competitive speciation; stochastic environment; environmental correlation; autocorrelation; competitive exclusion

INTRODUCTION

Evolutionary branching is a process by which a phenotypically monomorphic population gradually splits into two subpopulations. Theory has established that frequency-dependent selection can drive directional evolution towards a fitness minimum, where selection becomes disruptive and evolutionary branching may be initiated (Brown and Pavlovic 1992; Abrams et al. 1993; Metz et al. 1996; Geritz et al. 1998). It has also been shown that evolutionary branching may be driven by a variety of ecological interactions, e.g. competition, predation and mutualism (Doebeli and Dieckmann 2000), which underlines its potential importance for the generation of biological diversity.

For asexual organisms there are in principle no objections to the idea that evolving lineages could split through a process of evolutionary branching, resulting in two, or several, ecologically differentiated lineages. For sexual species, however, ecological differentiation is counteracted by repeated mixing of genotypes through recombination. It has been suggested that disruptive selection in sexual populations can select for assortative mating within diverging lineages such that speciation, either in sympatry or parapatry, becomes possible. Under what circumstances this kind of speciation process is likely or even possible is much debated and treated in a number of papers (Gourbiere 2004; Matessi et al. 2001; Polechova and Barton 2005; Ripa 2008; Waxman and Gavrilets 2005). Rather than treating the problem of reproductive isolation we will here focus on the ecological mechanisms involved in a branching process, relevant for sexual and asexual organisms alike.

From an ecological point of view, the crucial condition for branching to occur is coexistence of a resident and a mutant phenotype. So called branching points are hence characterized not only as convergent stable fitness minima but also by the mutual invasibility of morphs with strategy values in its vicinity (Metz et al. 1996; Geritz et al. 1998). The fact that two diverging morphs are mutually invasive does however not guarantee their coexistence if stochastic population growth is taken into account. During the initial phase of the branching the two morphs are very similar, with large niche overlap, and can be expected to compete strongly with each other. Strong competition easily leads to highly variable population sizes if stochasticity is allowed (May 1973), maybe even to the extent that one of the morphs goes extinct and branching has to start anew. Demographic stochasticity can severely delay branching of small populations (Metz et al. 1996; Claessen et al. 2007). If the two morphs experience uncorrelated environments during the initial stages of divergence it is likely that one of the two occasionally grows in density and drives the other one to extinction, which thereby impedes the branching process. However, two ecologically similar morphs are likely to experience environmental fluctuations in similar ways. It follows that the environmental correlation should be strong during the initial branching and decline as the ecological divergence progresses. Johansson and Ripa (2006) studied the effects of environmental fluctuations on the branching of large populations. They showed that the likelihood for branching depends on the relative rates at which competition and environmental correlation declines during branching. If environmental correlation declines faster than competition, the resulting relatively low correlation in growth rates of the strongly competing morphs can severely hamper branching through repeated stochastic extinctions. It is still unclear, however, under what circumstances environmental correlation can be considered to decline faster or slower than competition, as two morphs differentiate. Compared to Johansson and Ripa (2006) we here use a more mechanistic model of both competition and environmental fluctuations, which allows for stronger conclusions and more useful interpretations of the results. We study the branching of a consumer species feeding on two alternative resources with explicit dynamics. Environmental fluctuations enter through the growth rates of the resources. These ecological, relatively fast fluctuations are assumed not to affect the evolutionary dynamics of the system however, e.g. by influencing the invasion fitness of a rare morph. In addition to environmental correlation, we also study the effects of environmental autocorrelation, which is known to play an important role for the extinction risk of single populations (Petchey et al. 1997; Ripa and Lundberg 1996), as well as for the dynamics and extinction risks of interacting species (Caswell and Cohen 1995; Ripa and Ives 2003; Ripa et al. 1998). We find that branching will be impeded or at least delayed if the environmental fluctuations in resource growth rates have little or negative correlation. The same effect is found for a positive temporal autocorrelation of the environment and especially if the two conditions are combined will branching be impeded. We also show that the model can exhibit cycles of branching and extinction under the influence of environmental fluctuations.

METHODS

We study a model of consumers feeding from two resource species. This is a well studied scenario for evolutionary branching (Diekmann et al. 2005; Egas et al. 2004; Rueffler et al. 2006) which we here adapt to include effects of environmental fluctuations. For simplicity, we assume that the resource populations have fast dynamics compared to the environment and the consumer population(s). Thus, on the short time scale the environment and the consumer population size are assumed to be fixed and the resource population will reach an equilibrium density corresponding to current circumstances. The (continuous time) growth of the resource populations is modelled as logistic growth with linear consumer functional responses:

$$\frac{dR_i}{d\tau} = R_i(\tau)\left(r_0 e^{\varepsilon_i} - bR_i(\tau) - \sum_{j=1}^{n} a_{ij} C_j \right), i = 1, 2 \tag{1}$$

where $R_i(\tau)$ is the size of resource population i at time τ, r_0 is its intrinsic growth rate, b represents strength of resource density dependence, a_{ij} is the attack rate of consumer j on resource i, and C_j is the density of consumer j ($j = 1..n$). Finally, ε_i is a stochastic, normally distributed, environmental factor with zero mean, which affects the growth of resource i.

The equilibrium resource densities, R_i^* ($i = 1, 2$), are readily obtained by calculating the positive solutions to $\frac{dR_i}{d\tau} = 0$. If no positive solution is found, which may happen at high consumer densities, $R_i^* = 0$ is used instead. In these cases it is assumed that the resource population will recover to positive numbers in consecutive time steps, e.g. through immigration or dormant life stages.

On the longer time scale (denoted by t instead of τ), we assume discrete time consumer dynamics according to:

$$C_{j,t+1} = C_{j,t}\left(1 - d + \lambda a_{1j} R_1^*(t) + \lambda a_{2j} R_2^*(t)\right) \tag{2}$$

where λ is a conversion factor from resources to consumers and d corresponds to the minimal amount of resources a consumer individual needs to exactly replace itself from one time-step to the next, either through survival or reproduction. Eq. (2) is truncated such that negative consumer densities correspond to extinction.

Attack rates (a_{ij}) are controlled by an evolving trait z scaled such that $z = Z_i$ corresponds to maximal specialization on resource species i ($i = 1,2$. $Z_1 = -1$ and $Z_2 = +1$). The attack rate a_{ij} of a consumer j with trait z_j on resource i declines with distance in trait space according to a Gaussian function:

$$a_{ij} = a(z_j, Z_i) = a_0 e^{-\frac{(z_j - Z_i)^2}{2\sigma_a^2}} , \tag{3}$$

where a_0 is maximal attack rate and σ_a controls the niche width of consumers; the larger σ_a the more efficiently a consumer can feed on both resources simultaneously. Alternatively, σ_a can be interpreted in terms of a trade-off in the consumption of the two resources, such that a small (large) σ_a corresponds to a strong (weak) trade-off. The eco-evolutionary scenario considered here is depicted in figure 1 for a single consumer population, for reference.

Without loss of generality we measure time (τ), resource densities (R_i) and consumer densities (C_j) in units such that $r_0 = 1$, $b = 1$ and $\lambda = 1$. The population dynamics are then completely controlled by the three parameters d, a_0 and σ_a, save for the stochastic dynamics of the environmental factors $\varepsilon_{i,t}$ (see below).

We obtain the resource equilibrium densities as:

$$R_i^*(t) = e^{\varepsilon_{i,t}} - \sum_{j=1}^{n} a_{ij} C_{j,t} . \tag{4}$$

Substituting eq. (4) into eq. (2) gives the consumer dynamics:

$$C_{j,t+1} = C_{j,t}\left(1 - d + a_{1j}\left(e^{\varepsilon_{1,t}} - \sum_{k=1}^{n} a_{1k} C_{k,t}\right) + a_{2j}\left(e^{\varepsilon_{2,t}} - \sum_{k=1}^{n} a_{2k} C_{k,t}\right)\right) \tag{5}$$

In deterministic models ($\varepsilon_{1,t} \equiv \varepsilon_{2,t} \equiv 0$), evolutionary branching may occur in this scenario (Diekmann et al. 2005; Egas et al. 2004; Rueffler et al. 2006). We analyze the evolutionary dynamics of the deterministic model here using the adaptive dynamics framework (Dieckmann and Law 1996; Geritz et al. 1998; Metz et al. 1996). We thus express the fitness w of an arbitrary consumer individual with trait value z' in a community of n monomorphic consumer populations as:

$$w(z',\mathbf{z},\mathbf{C}) = 1 - d + a(z',Z_1)\left(1 - \sum_{k=1}^{n} a(z_k,Z_1)C_k\right) + a(z',Z_2)\left(1 - \sum_{k=1}^{n} a(z_k,Z_2)C_k\right), \qquad (6)$$

where $\mathbf{z} = [z_1,\ldots,z_n]$ and $\mathbf{C} = [C_1,\ldots,C_n]$ are vectors of resident z-values and population sizes, respectively. The growth rate of consumer population i is consequently given by $w(z_i, \mathbf{z}, \mathbf{C})$ and equilibrium population sizes, $\mathbf{C}^*$, are found by solving :

$$w(z_i,\mathbf{z},\mathbf{C}^*) = 1 \text{, for all } i. \qquad (7)$$

The evolutionarily singular points of the monomorphic system ($i = 1$) can be found by studying the fitness gradient (Geritz et al. 1998; Metz et al. 1996) which, assuming ecological equilibrium, unfolds as:

$$g(z) = \left.\frac{\partial w(z',z,\mathbf{C}^*(z))}{\partial z'}\right|_{z'=z} = \frac{d}{\sigma_a^2}\left(-z + \frac{c^{2z} - c^{-2z}}{c^{4z} + c^{-4z}}\left(2\frac{a_0}{d}c^{z^2+1} - \left(c^{2z} + c^{-2z}\right)\right)\right), \qquad (8)$$

where $c = e^{-\frac{1}{2\sigma_a^2}}$. It is straightforward to show that the generalist strategy ($z = 0$) is a branching point, i.e. a convergent stable fitness minimum, if

$$\frac{2c}{2 - \sigma_a^2} > \frac{d}{a_0} \text{ and } \sigma_a < 1. \qquad (9)$$

We are here interested in the process of evolutionary branching and choose parameter values accordingly. By studying fitness gradients of the dimorphic system we established that the system eventually will converge to an ESS (Evolutionarily Stable State), with symmetric trait values, $z_1 = -z_2 = z^*$ (not shown for brevity). For all illustrations we use $d = 1.2$, $a_0 = 1.8$ and $\sigma_a = 0.85$, which assures positive, stable equilibrium resource and consumer abundances for all relevant z-values but still allows for consumer extinction at low resource levels ($d > 1$).

Environmental fluctuations

Environmental fluctuations are built into the model as fluctuations of the intrinsic growth rates of the resource species through the stochastic variables $\varepsilon_{i,t}$, $i = 1,2$ (eqs. 1, 4, 5). We let ρ denote the correlation between $\varepsilon_{1,t}$ and $\varepsilon_{2,t}$ such that fluctuations are fully correlated at $\rho = 1$ and totally uncorrelated at $\rho = 0$. A positive ρ is likely if a common external factor, such as temperature, affects both resources in a similar way. If, on the other hand, the resource species have non-overlapping temperature niches a zero or even negative correlation is expected.

To investigate the possible role of environmental autocorrelation we let our model environments vary according to a first order autoregressive model (Box and Jenkins 1970):

$$\varepsilon_{i,t+1} = \gamma \varepsilon_{i,t} + \mu_{i,t}\ , \ i = 1,2, \tag{10}$$

where γ ($-1 < \gamma < 1$) controls the strength of autocorrelation of both environments. A γ close to one represents a heavily autocorrelated environment, close to a random walk, whereas $\gamma = 0$ corresponds to white noise. Many abiotic environmental factors are known to show positive temporal autocorrelation (Pimm and Redfearn 1988; Steele 1985). Also the biotic environment is known to change only slowly over time (Lawton 1988). Negative autocorrelation is perhaps less likely for natural environments but we include it in the analysis for completeness. $\mu_{i,t}$ ($i = 1, 2$; $t = 0, 1, \ldots$) is a set of serially uncorrelated (white noise), normally distributed random variables with zero mean and variance σ_μ^2. Setting $\sigma_\mu^2 = \sigma_\varepsilon^2\left(1-\gamma^2\right)$ assures that the stationary variances of the environmental processes $\varepsilon_{i,t}$ are equal to σ_ε^2, irrespective of γ (Box and Jenkins 1970). Finally, we set corr($\mu_{1,t}$, $\mu_{2,t}$) = ρ which renders corr($\varepsilon_{1,t}$, $\varepsilon_{2,t}$) = ρ as well, as long as γ is the same for both environments (Moran 1953).

Estimation of extinction risks

The exact extinction risk of a model population can normally only be calculated through computer simulations. From the linearized population dynamics one may however estimate the coefficient of variation (*CV*) which gives the relative variability in population densities. Here we will use population *CV* as a proxy for extinction risk (May 1973), and later compare analytical results with numerical simulations. The linear approximations and *CV* calculations are presented in Appendix A.

RESULTS

We will in the following study how correlation and autocorrelation in the environmental fluctuations affect variability in consumer populations during evolutionary branching. By comparing extinction risks of a single consumer and extinction risks in coalitions of two consumer strategies we will elucidate how evolutionary branching can be affected by environmental fluctuations. If extinction risk is low for a single species at the branching point but high for populations of the two newly formed morphs, branching can be impeded or at least delayed. Therefore we will study in detail the *relative* increase in extinction risk during branching, when a single morph splits into two. For completeness we will also study extinction risks during the whole diversification process; starting from a single consumer evolving towards the branching point until the dimorphic ESS is finally reached. Specifically, we will envision an idealized evolutionary process where a single strategy initiated as a specialist consumer evolves towards $z = 0$ and gives rise to two strategies symmetrically distributed around zero ($z_1 = -z_2$ for consumer strategies 1 and 2) which subsequently diverge in trait space until $z_1 = -z_2 = z^*$. For convenience the single species is also assumed to start at $z = z^*$.

We start by studying a case without autocorrelation of the environmental fluctuations ($\gamma = 0$). The approximate *CV* for a single species is calculated as (Appendix A):

$$CV_I^2 \approx \sigma_\varepsilon^2 \frac{a_1^2 + a_2^2 + 2\rho a_1 a_2}{1-\left(1+d-a_1-a_2\right)^2}, \tag{11}$$

where a_1 and a_2 are the attack rates on the first and second resources, respectively. We note in passing that the *CV* increases with the environmental correlation, ρ. A reliance on two uncorrelated resources gives a consumer an advantage in terms of a decreased variability in total resource abundance, the so called portfolio effect, but this advantage dwindles as the resources become increasingly correlated.

We now calculate the *CV* of the dimorphic case. With the symmetry as described above, the system can be described by a single trait value $z = z_1 = -z_2$. We write attack rates of the two species according to $a_{11} = a_{22} = a_1$ and $a_{12} = a_{21} = a_2$ where $a_1 = \exp\left(-\left(z-1\right)^2/2\sigma_a^2\right)$ and $a_2 = \exp\left(-\left(z+1\right)^2/2\sigma_a^2\right)$, which gives the following expression for the *CV* (Appendix A, substitute $\gamma = 0$ in eq. A17):

$$CV_{II}^2 \approx \frac{\sigma_\varepsilon^2}{2C_{II}^*}\left(\frac{\left(1+\rho\right)}{2-C_{II}^*\left(a_1+a_2\right)^2} + \frac{\left(1-\rho\right)}{2-C_{II}^*\left(a_1-a_2\right)^2}\right), \tag{12}$$

where C_{II}^* is the equilibrium population size of both consumer populations in the deterministic model.

In figure 2 the CV_I and CV_{II} from eqs. (11) and (12) are plotted for $\rho = 0$ along with estimated values from simulations. As a single consumer starting out from $z = z^*$ evolves towards the branching point, CV_I decreases due to an increased portfolio effect – the consumer becomes less and less dependent on a single resource and can compensate a low level of resources by consuming the other. After branching, however, the CV is higher due to the competition between the newly formed morphs. CV_{II} remains roughly constant as z grows from 0 to z^* after branching. Since competition decreases during divergence the dynamics become increasingly similar to that of a single species, which is reflected by the decreasing difference between CV_I and CV_{II}.

As shown in figure 2 there is a difference between CV_I and CV_{II} at $z = 0$ and if this difference is large one may expect branching to be impeded. Following Johansson and Ripa (2006) an estimate of CV immediately after branching is obtained by letting the symmetric trait values z_1 and z_2 go to zero. As the trait values approaches zero so does the difference between a_1 and a_2. Starting with the two species case we obtain the limit directly from eq. (12):

$$\lim_{z\to 0} CV_{II}^2 \approx \frac{\sigma_\varepsilon^2}{2C_{II}^*}\left(\frac{1+\rho}{1+(1+d-2a)}+\frac{1-\rho}{2}\right), \tag{13}$$

where a corresponds to the attack rates at $z = 0$, for which $a = a_1 = a_2$. We note here that the expression in (13) really should be regarded as a limit case, even though it can be obtained directly from (12) by setting $z = 0$. The dynamics of the two consumers become degenerate in the limit as the two populations become ecologically equivalent. If the fluctuations in consumer population densities would be independent from each other, this would lead to a *CV* approaching infinity with rapid extinction of one population as a result. However, as the consumers become more and more similar, they also respond to fluctuations in resource abundance in an increasingly similar fashion. This synchronization of their stochastic growth rates counterbalances the increased instability due to the increasing competition and the end result is a CV_{II} which smoothly approaches a limiting value as z goes to zero (cf. Johansson and Ripa 2006).

For the single species case we get, after some simplification:

$$CV_I^2(z=0) \approx \frac{\sigma_\varepsilon^2}{C_I^*}\frac{1+\rho}{1+(1+d-2a)} \tag{14}$$

The ratio between (the square of) these two coefficients of variation gives a measure of how much extinction risk may increase during branching:

$$q = \lim_{z\to 0}\frac{CV_{II}^2}{CV_I^2} \approx 1+\frac{1}{2}\left(1+(1+d-2a)\right)\frac{1-\rho}{1+\rho} \tag{15}$$

The ratio q is a decreasing function of ρ, i.e. the more correlated environments the smaller extinction risk after branching. For fully correlated environments ($\rho = 1$) we get $q = 1$, i.e. no difference in extinction risk during the transition from one to two species. As ρ approaches –1 the ratio goes to infinity which means that a negative correlation should be particularly disadvantageous for branching. Note that a negative environmental correlation here does not imply that the growth rates of the two consumers are negatively correlated shortly after branching, since they to a large extent feed on the same resources.

The expression $(1 + d - 2a)$ in eq. (15), hereafter denoted h as in Appendix A, corresponds to the slope of the single species recruitment function at equilibrium. For stability, it is required that $-1 < h < 1$. It follows that the ratio q is the largest when h is close to +1, i.e. when the density regulation of consumers is weak.

To sum up the analytical results, we conclude that a low or negative correlation in the environment gives an increased extinction risk, especially in combination with weak density regulation.

Simulations without autocorrelation

Computer simulations (see Appendix B for details) both confirm and contradict the analytical results above. First of all, for relatively low environmental variation, the CV of simulated populations fit well with the analytical predictions (Fig. 2). The CV of each of the two species is relatively constant during the evolutionary divergence following branching, suggesting that the dimorphic ESS should be reached as long as branching is possible. However, when environmental variation is increased so that extinctions may occur, extinction risk measured from simulations increase considerably along the z axis both for a single species and for two species (Fig. 3A). The increased extinction risk can be understood by comparing the population dynamics of generalists and specialists in phase space. Figures 3B and C show the dynamics of two competing consumer types together with the probability that one of them goes extinct in the next time step. Note that high population densities lead to extinctions in our model (due to depletion of resources [eq. 4]). The relative variation in population densities is similar in the two cases, but it is clear that generalists face a lower extinction risk of than specialists. Firstly, the relative distance between mean population density and densities where extinctions occur is larger for a generalist than a specialist. Two generalist types are less efficient consumers than two specialist types and it therefore takes more of them to deplete all resources. Secondly, the strongly competing generalists have negatively correlated population densities, whereas the risk of extinction is high when total population density is high (Fig. 3B). Both these mechanisms contribute to a lower total extinction risk for generalists, as compared to specialist types which have relatively independent population dynamics (the distribution of population densities is almost circular) and independent extinction risks (Fig 3C). In conclusion, even though population *CV* is similar in the two cases, the risk of extinction is severely elevated for specialists.

For a single species, a similar effect occurs; also here the distance from mean population densities to critically high densities is larger for generalists than for specialists. In addition, the *CV* is higher for specialists in this case (Fig 2).

The simulations in Figure 3 are all carried out with uncorrelated resource growth ($\rho = 0$). Changes in the correlation parameter alter the *CV* of population densities (eqs. 11 and 12) as well as the shape of their distributions, which affects the risk of extinction. As an example, increasing the environmental correlation of two close competitors (Fig. 3B), would make the distribution of population densities more positively correlated, and thereby increase the risk that the populations reach fatal densities. Simulations show, however, that environmental correlation (positive or negative) will not change the observed pattern of increased extinction risk with increased specialisation (not shown). The reason is that although the stationary distribution of population densities changes, the risk of extinction from any given point in phase space remains the same. The relative distance between mean population densities and densities with high risk of extinction therefore remains shorter for specialists.

The increased extinction risk during divergence may result in a pattern of recurrent evolutionary branching and extinction as shown in figure 3C. If one of the species goes extinct during dimorphic divergence the remaining species will evolve back towards the branching point where a dimorphism may be re-established and start the divergence again. The remaining single species is however initially also subject to a large extinction risk (Fig. 3A), and may go extinct itself which ends the evolutionary cycle (Fig. 3D).

The pattern of recurrent branching and the likelihood that it occurs depends on the level of the environmental variance, σ_ε^2, and other parameters. In some cases, for example, the pattern cannot be sustained as the remaining species do not evolve back to the branching point but get trapped at an alternative, local single species ESS (not shown). Although we have not investigated this in any great detail, the pattern of repeated branching, in different guises, can be observed in evolutionary simulations of this model for a significant portion of parameter space.

Autocorrelation and impeded branching

Environmental autocorrelation has, as we shall see, potentially a large influence on the branching process. As above, we use the linearized population dynamics as a first step to calculate approximations for population *CV* as a proxy for extinction risk.

Figure 4A shows how the *CV* changes along the z-axis when fluctuations are heavily autocorrelated ($\gamma = 0.95$). Single species *CV* decreases during evolution towards the branching point just like in figure 2. Two species *CV* however, is very large precisely after branching and decreases thereafter. In this case the *CV* is a more accurate predictor of extinction risks (Fig. 4B). Compared to the case without autocorrelation (Fig. 2, 3A) there are thus two differences. Firstly, for the two species case the extinction risks decreases with z, which is just the opposite to the case without autocorrelation (Fig. 3A). Secondly, the difference in *CV* between the two-species model and the single species model close to $z = 0$ is much larger than before.

As above, we calculate the ratio between the single-species *CV* and two-species *CV* at the branching point ($z = 0$), which simplifies to (Appendix A):

$$q = \frac{CV_{II}^2(z=0)}{CV_I^2(z=0)} \approx 1 + \frac{1}{2}(1+h)\left(\frac{1-\rho}{1+\rho}\right)\left(\frac{1+\gamma}{1-\gamma}\right)\left(\frac{1-h\gamma}{1+h\gamma}\right) \tag{16}$$

From eq. (16) it is apparent that q approaches infinity as the environmental autocorrelation γ approaches 1, which is its maximal value. Also, we note that the effects of density dependence h and environmental correlation ρ remain (cf. eq. 15), and that there is an interaction between h and γ. The interaction is such that q is larger if h and γ have opposite sign. Since only non-negative γ-values are considered here, the interaction will amplify q if h is negative, which corresponds to strong density dependence. However, a negative h will also decrease the factor $(1 + h)$, which makes the dependence on h somewhat more complicated compared to eq. (15).

The strong effect of environmental autocorrelation on population variability just after branching can be understood by contemplating the nature of the environmental fluctuations and their effects on the population dynamics. First of all, asymmetric fluctuations of the two resources give one consumer or the other the upper hand. If these fluctuations are positively autocorrelated, one of the competitors will have the advantage long enough to push the other down to low densities, or even extinction. It is also clear that this effect is the strongest if the resources commonly fluctuate in an asymmetric way, i.e. if environmental variability is uncorrelated or even negatively correlated. In more technical terms, the effects of a positive autocorrelation can be understood from the eigenvalues of the Jacobian of the two-species system (see Appendix A, Ripa and Ives 2003). A system of two strongly competing populations will have (at least) one eigenvalue which is close to +1, which renders large fluctuations in an autocorrelated environment, especially if the environmental fluctuations have low or negative correlation (Ripa and Ives 2003). Lastly, we note that the effects of correlation ρ and autocorrelation γ are multiplicative, which makes the combination of a low or negative correlation and a high autocorrelation particularly severe.

The evolutionary consequence of the increased extinction risk shortly after branching may be extinction of one of the newly formed branches and impeded branching, as illustrated by figure 4C.

DISCUSSION

We have studied how extinction risks during evolutionary branching are influenced by correlation and autocorrelation in environmental fluctuations. In our model system we find two different extinction scenarios, with different ecological mechanisms and hence different dependence on environmental correlation and autocorrelation.

Firstly, populations can go extinct from high population densities after resource depletion. A high resource availability in one time step yields high population size which in turn leads to strong *intraspecific* competition if resource regrowth is low in the next time step. This type of extinction from high population densities is possible especially if a population has strong density dependence as has been demonstrated in theory (Petchey et al. 1997; Ripa and Lundberg 1996; Ripa and Lundberg 2000; Roughgarden 1975) as well as field experiments (Klemola et al. 2000). In our model these extinctions occur for a single consumer as well as two competitors, but are most likely when a consumer (alone or with a symmetric competitor) is specialized on a single resource (Fig. 3A), since a specialist (by definition) is a more efficient consumer (Fig. 3C). Correlated growth rates of the resources can affect the likelihood of this type of extinctions by changing the degree of variation in population densities and the shape of their distributions in relation to the density dependent extinction risks. Temporal autocorrelation of the environment also has a major effect on this type of extinction – it is only likely when autocorrelation is low (compare Figs. 3A and 4B). A highly autocorrelated environment, which only changes slowly over time, is more easily tracked by the consumer and does not cause such sudden shortages of resources.

In the scenario studied here, the degree of specialization increases for the two diverging consumer after branching. As a consequence the risk of extinction from high population sizes, described above, increases as well. For sufficient environmental variability evolution may thus lead to extinction and even result in cycles of branching and extinction (Fig. 3C). Evolution towards extinction may seem counterintuitive but occurs in many models where ecological feedback is taken into account as a driving factor in the evolutionary dynamics (Gyllenberg et al. 2002; Matsuda and Abrams 1994; Parvinen 2005). Also patterns of repeated branching have been shown to appear in various model scenarios (Dercole 2003; Doebeli and Dieckmann 2000; Ito and Dieckmann 2007; Kisdi et al. 2001). In the cited studies evolution to extinction occurs either deterministically or as an effect of evolutionary or demographic stochasticity. Our results show that also environmental fluctuations can result in such evolution and, as a consequence, lead to branching-extinction cycles. These phenomena depend strongly on the nature of the density dependence, which in the case of our model is such that the risk of going extinct increases with specialisation. Other models may give different predictions.

Secondly, extinctions may occur due to stochastic demographic events when population densities are small. Such critically small densities are caused by *interspecific* competition which is strongest close to branching points (Figs. 4A, B). Asymmetric resource fluctuations, if they occur, give an advantage to one consumer over the other. If the asymmetry is severe enough and lasts for long enough time, the disfavoured consumer can be driven all the way to extinction. It follows that low or negative environmental correlation and a high autocorrelation makes these conditions more likely to occur. A negative correlation causes frequent, strong asymmetries and a high autocorrelation makes them last for a long time.

This kind of extinction may, as shown by figure 4C, impede or at least delay branching. Our results confirm the finding in Johansson and Ripa (2006) that quickly decreasing correlation in trait space, which here occurs for little or, in particular, negatively correlated resources, can give a large relative increase in extinction risk during branching (eq. 18). With autocorrelated environmental fluctuations, the effect of low correlation is aggravated since autocorrelation and correlation affect the relative increase in extinction risk multiplicatively (eq. 21).

The result that low environmental correlation causes extinction just after branching is also consistent with the findings of Claessen et al. (2007), who studied the effects of demographic stochasticity on the branching process. Demographic stochasticity is most prominent at low population sizes (MacArthur and Wilson 1967), but also by definition uncorrelated between species. It follows that small populations could be prevented from branching by demographic stochasticity alone, which is exactly what Claessen and co-workers found.

In contrast to the branching-extinction cycles described above, which depend on particular relationships between specialization and density dependence, the effects of a high autocorrelation and a low correlation should be more generally applicable to scenarios of competitive branching. This prediction is amenable to experimental tests, e.g. in radiations in laboratory microcosms. Massin and Gonzalez (2006) let bacteria radiate under different disturbance regimes, and found delayed diversification when the disturbances were more aggregated in time, i.e. more autocorrelated. Although the type of disturbance they used (mixing of the whole system) is not directly comparable to the kind of environmental fluctuations we have envisioned here, the theoretical and empirical evidence point in the same direction.

In our study we assume that the ecological timescales can be separated from the evolutionary timescales and that morphs diverge symmetrically, starting exactly from the branching point. It would be interesting to investigate the effects of relaxing these two assumptions. Slow environmental fluctuations that are visible on an evolutionary timescale would for example affect the position of the branching point and the shape of coexistence regions around it (Metz et al. 1996). Asymmetric trait values would lead to asymmetric competition with various effects on population fluctuations and extinction risks. Obviously, branching driven by other ecological interactions than resource competition, e.g., mutualism or predator-prey interactions, may be affected differently by environmental fluctuations. Environmental variation may also enter population dynamics in other ways, depending on the scenario envisioned. Although these examples show that a number of questions regarding branching in stochastic environments remain to be addressed, the ecological mechanisms investigated here are of very general nature. We therefore believe these results are broadly applicable and contribute to an increased understanding of the possible role of environmental fluctuations for the process of evolutionary branching or even speciation.

ACKNOWLEDGEMENTS

This research was supported by the Swedish Research Council. We are grateful to J. Brown, P. Lundberg and N. Jonzén for advice and comments on earlier drafts of this manuscript.

APPENDIX A: CALCULATIONS OF CV

Here we derive the approximations for the *CV* of the consumer populations. We use the complete environmental model from start, including both environmental correlation and autocorrelation.

Single species case

First, we analyze the single consumer version of eq. (5):

$$C_{t+1} = f_I(C_t, \varepsilon_{1,t}, \varepsilon_{2,t}) = C_t\left(1 - d + a_1\left(e^{\varepsilon_{1,t}} - a_1 C_t\right) + a_2\left(e^{\varepsilon_{2,t}} - a_2 C_t\right)\right) \tag{A1}$$

The non-zero deterministic equilibrium density of a single consumer, C_I^*, amounts to:

$$C_I^* = f\left(C_I^*, 0, 0\right) \Leftrightarrow C_I^* = \frac{a_1 + a_2 - d}{a_1^2 + a_2^2} \tag{A2}$$

Next, we linearize eq. (A1) at the deterministic equilibrium, which gives:

$$x_{t+1} = hx_t + k_1\varepsilon_{1,t} + k_2\varepsilon_{2,t} \tag{A3}$$

where

$$x_t = C_t - C_I^*, \tag{A4a}$$

$$h = \left.\frac{\partial f_I}{\partial C}\right|_{\substack{C=C_I^* \\ \varepsilon_1=\varepsilon_2=0}} = 1 + d - a_1 - a_2, \tag{A4b}$$

and

$$k_i = \left.\frac{\partial f_I}{\partial \varepsilon_i}\right|_{\substack{C=C_I^* \\ \varepsilon_1=\varepsilon_2=0}} = a_i C_I^*. \tag{A4c}$$

The expression $k_1\varepsilon_{1,t} + k_2\varepsilon_{2,t}$ in eq. (A3) is a weighted sum of the two resource environments, which are possibly both correlated and autocorrelated. However, they are both AR(1) processes (eq. 10) and share the same autocorrelation parameter γ, which simplifies things considerably. It follows readily that $k_1\varepsilon_{1,t}+k_2\varepsilon_{2,t}$ is equivalent to a single AR(1) process with the same parameter γ. By assumption $\mathrm{V}(\varepsilon_{1,t})=\mathrm{V}(\varepsilon_{2,t})=\sigma_\varepsilon^2$ and $\mathrm{Cov}(\varepsilon_{1,t},\varepsilon_{2,t})=\rho\sigma_\varepsilon^2$, which gives:

$$V(k_1\varepsilon_{1,t}+k_2\varepsilon_{2,t})=k_1^2V(\varepsilon_{1,t})+k_2^2V(\varepsilon_{2,t})+2k_1k_2Cov(\varepsilon_{1,t},\varepsilon_{1,t})=C_I^{*2}\sigma_\varepsilon^2\left(a_1^2+a_2^2+2a_1a_2\rho\right)$$

The stochastic dynamics of x_t in (A3) is an AR(1) process with AR(1) noise. Its stationary variance is then given by (Ripa and Heino 1999):

$$\mathrm{V}(x_t)=\frac{1+h\gamma}{(1-h^2)(1-h\gamma)}V(k_1\varepsilon_{1,t}+k_2\varepsilon_{2,t})=\left(\frac{1+h\gamma}{1-h\gamma}\right)\frac{C_I^{*2}\sigma_\varepsilon^2\left(a_1^2+a_2^2+2a_1a_2\rho\right)}{1-h^2}$$

Finally, we can calculate the squared *CV* of a single consumer population:

$$CV_I^2=\frac{\mathrm{V}(C_t)}{\mathrm{E}(C_t)^2}\approx\frac{\mathrm{V}(x_t)}{C_I^{*2}}=\left(\frac{1+h\gamma}{1-h\gamma}\right)\frac{\sigma_\varepsilon^2\left(a_1^2+a_2^2+2a_1a_2\rho\right)}{1-h^2}, \tag{A5}$$

where E() denotes the stationary mean.

We note here that a generalist strategy ($z = 0$) has $a_1 = a_2 = a$, which gives:

$$CV_I^2[z=0]\approx\left(\frac{1+h\gamma}{1-h\gamma}\right)\frac{\sigma_\varepsilon^2 2a^2(1+\rho)}{1-h^2}=\left[2a^2=\frac{2a-d}{C_I^*}=\frac{1-h}{C_I^*}\right]=\frac{\sigma_\varepsilon^2}{C_I^*}\left(\frac{1+h\gamma}{1-h\gamma}\right)\frac{(1+\rho)}{1+h} \tag{A6}$$

Two consumers

Next, we analyze the dynamics of two consumers positioned symmetrically around the generalist strategy ($z_1 = -z_2$). The symmetry implies symmetric attack rates: $a_{11} = a_{22} = a_1$ and $a_{12} = a_{21} = a_2$:

$$\begin{cases} C_{1,t+1} = f_{II,1}\left(C_{1,t}, C_{2,t}, \varepsilon_{1,t}, \varepsilon_{2,t}\right) \\ C_{2,t+1} = f_{II,2}\left(C_{1,t}, C_{2,t}, \varepsilon_{1,t}, \varepsilon_{2,t}\right) \end{cases} = \\ = \begin{cases} C_{1,t+1} = C_{1,t}\left(1 - d + a_1\left(e^{\varepsilon_{1,t}} - a_1 C_{1,t} - a_2 C_{2,t}\right) + a_2\left(e^{\varepsilon_{1,t}} - a_2 C_{1,t} - a_1 C_{2,t}\right)\right) \\ C_{2,t+1} = C_{2,t}\left(1 - d + a_2\left(e^{\varepsilon_{1,t}} - a_1 C_{1,t} - a_2 C_{2,t}\right) + a_1\left(e^{\varepsilon_{1,t}} - a_2 C_{1,t} - a_1 C_{2,t}\right)\right) \end{cases} \tag{A7}$$

The non-zero deterministic equilibrium densities are equal due to the symmetry and given by:

$$\begin{cases} C_{II}^* = f_{II,1}\left(C_{II}^*, C_{II}^*, 0, 0\right) \\ C_{II}^* = f_{II,2}\left(C_{II}^*, C_{II}^*, 0, 0\right) \end{cases} \Leftrightarrow C_{II}^* = \frac{a_1 + a_2 - d}{\left(a_1 + a_2\right)^2} \tag{A8}$$

As above, we continue by linearizing the dynamics in (A7) at the deterministic equilibrium which gives:

$$\mathbf{x}_{t+1} = J\mathbf{x}_t + K\boldsymbol{\varepsilon}_t \tag{A9}$$

where $\mathbf{x}_t = \begin{pmatrix} x_{1,t} \\ x_{2,t} \end{pmatrix} = \begin{pmatrix} C_{1,t} - C_{II}^* \\ C_{2,t} - C_{II}^* \end{pmatrix}$, the Jacobian *J* has elements:

$$J_{11} = J_{22} = \left.\frac{\partial f_{II,1}\left(C_1, C_2, \varepsilon_1, \varepsilon_2\right)}{\partial C_1}\right|_{\substack{C_1 = C_2 = C_{II}^* \\ \varepsilon_1 = \varepsilon_2 = 0}} = 1 - C_{II}^*\left(a_1^2 + a_2^2\right), \tag{A10a}$$

$$J_{12} = J_{12} = \left.\frac{\partial f_{II,1}\left(C_1, C_2, \varepsilon_1, \varepsilon_2\right)}{\partial C_2}\right|_{\substack{C_1 = C_2 = C_{II}^* \\ \varepsilon_1 = \varepsilon_2 = 0}} = -2C_{II}^* a_1 a_2, \tag{A10b}$$

and the elements of the matrix *K* are:

$$K_{11} = K_{12} = C_{II}^* a_1$$

$$K_{12} = K_{21} = C_{II}^* a_2$$

The system (A9) is most easily analyzed by a diagonalization, i.e. by transforming the coordinates to the eigenvectors of the Jacobian J (e.g. Ripa and Ives 2003). The eigenvalues of J are given by:

$$\lambda_1 = 1 - C_{II}^*\left(a_1 + a_2\right)^2 \tag{A11a}$$

$$\lambda_2 = 1 - C_{II}^*\left(a_1 - a_2\right)^2 \tag{A11b}$$

and the corresponding, normalized, eigenvectors are:

$$\mathbf{v}_1 = \frac{1}{\sqrt{2}}\left(1,1\right)^T \tag{A12a}$$

$$\mathbf{v}_2 = \frac{1}{\sqrt{2}}\left(1,-1\right)^T \tag{A12b}$$

Transforming $x_{1,t}$ and $x_{2,t}$ to the orthogonal coordinate axes given by $\mathbf{v}_1$ and $\mathbf{v}_2$ gives the new coordinates $y_{1,t}$ and $y_{2,t}$:

$$y_{1,t} = \mathbf{v}_1^T\mathbf{x}_t = \frac{1}{\sqrt{2}}\left(x_{1,t} + x_{2,t}\right) \tag{A13a}$$

$$y_{2,t} = \mathbf{v}_2^T\mathbf{x}_t = \frac{1}{\sqrt{2}}\left(x_{1,t} - x_{2,t}\right) \tag{A13b}$$

Expressed in these new coordinates, the system in (A9) is transformed to two separate dynamic equations:

$$y_{1,t+1} = \lambda_1 y_{1,t} + \frac{1}{\sqrt{2}}\left(K_{11} + K_{12}\right)\left(\varepsilon_{1,t} + \varepsilon_{2,t}\right) \tag{A14a}$$

and

$$y_{2,t+1} = \lambda_2 y_{2,t} + \frac{1}{\sqrt{2}}\left(K_{11} - K_{12}\right)\left(\varepsilon_{1,t} - \varepsilon_{2,t}\right) \tag{A14b}$$

As above, we identify the external inputs in eqs. (A14a,b) as sums of two AR(1) processes with equal autocorrelation parameter (γ). Consequently, the variances of y_1 and y_2 can be calculated as:

$$\begin{aligned}
\mathrm{V}(y_{1,t}) &= \frac{1+\lambda_1\gamma}{(1-\lambda_1^2)(1-\lambda_1\gamma)}\mathrm{V}\left(\frac{1}{\sqrt{2}}(K_{11}+K_{12})(\varepsilon_{1,t}+\varepsilon_{2,t})\right) = \\
&= \left(\frac{1+\lambda_1\gamma}{1-\lambda_1\gamma}\right)\frac{(K_{11}+K_{12})^2}{(1-\lambda_1^2)}\frac{1}{2}\mathrm{V}(\varepsilon_{1,t}+\varepsilon_{2,t}) = \\
&= \left(\frac{1+\lambda_1\gamma}{1-\lambda_1\gamma}\right)\frac{C_{II}^{*\,2}(a_1+a_2)^2}{(1-\lambda_1^2)}\sigma_\varepsilon^2(1+\rho) = \left[C_{II}^*(a_1+a_2)^2 = 1-\lambda_1\right] = \\
&= \left(\frac{1+\lambda_1\gamma}{1-\lambda_1\gamma}\right)\frac{C_{II}^*}{(1+\lambda_1)}\sigma_\varepsilon^2(1+\rho)
\end{aligned} \qquad \text{(A15a)}$$

$$\mathrm{V}(y_{2,t}) = \ldots = \left(\frac{1+\lambda_2\gamma}{1-\lambda_2\gamma}\right)\frac{C_{II}^*}{(1+\lambda_2)}\sigma_\varepsilon^2(1-\rho) \qquad \text{(A15b)}$$

It follows from (A13a,b) and the fact that $\mathrm{V}(x_{1,t}) = \mathrm{V}(x_{2,t})$ by symmetry that $\mathrm{Cov}(y_{1,t}, y_{2,t}) = 0$. Thus, we have enough results to back-transform to the original coordinates:

$$\begin{aligned}
x_{1,t} &= \frac{1}{\sqrt{2}}(y_{1,t}+y_{2,t}) \Rightarrow \\
&\Rightarrow V(x_{1,t}) = V(x_{2,t}) = \frac{1}{2}\left(V(y_{1,t}) + V(y_{2,t}) + 2Cov(y_{1,t}, y_{2,t})\right) = \\
&= \frac{C_{II}^*\sigma_\varepsilon^2}{2}\left(\left(\frac{1+\lambda_1\gamma}{1-\lambda_1\gamma}\right)\frac{(1+\rho)}{(1+\lambda_1)} + \left(\frac{1+\lambda_2\gamma}{1-\lambda_2\gamma}\right)\frac{(1-\rho)}{(1+\lambda_2)}\right)
\end{aligned} \qquad \text{(A16)}$$

The *CV* of both consumers becomes:

$$CV_{II}^2 = \frac{V(C_{1,t})}{E(C_{1,t})^2} \approx \frac{V(x_{1,t})}{C_{II}^{*\,2}} = \frac{\sigma_\varepsilon^2}{2C_{II}^*}\left(\left(\frac{1+\lambda_1\gamma}{1-\lambda_1\gamma}\right)\frac{(1+\rho)}{(1+\lambda_1)} + \left(\frac{1+\lambda_2\gamma}{1-\lambda_2\gamma}\right)\frac{(1-\rho)}{(1+\lambda_2)}\right) \qquad \text{(A17)}$$

At $z = 0$, λ_1 becomes equal to h above (eq. A4b) and λ_2 becomes 1. Moreover, C_{II}^* becomes equal to $\frac{1}{2}C_I^*$. This taken together gives:

$$CV_{II}^2[z=0] \approx \frac{\sigma_\varepsilon^2}{C_I^*}\left(\left(\frac{1+h\gamma}{1-h\gamma}\right)\frac{(1+\rho)}{(1+h)}+\left(\frac{1+\gamma}{1-\gamma}\right)\frac{(1-\rho)}{2}\right) \tag{A18}$$

Finally, we can calculate the (squared) approximate ratio between the two-species *CV* (*CV*$_{II}$, eq. A18) and the single-species *CV* (*CV*$_I$, eq. A6) at the branching point $z = 0$, which simplifies to:

$$q = \frac{CV_{II}^2[z=0]}{CV_I^2[z=0]} \approx 1+\frac{1}{2}(1+h)\left(\frac{1-\rho}{1+\rho}\right)\left(\frac{1+\gamma}{1-\gamma}\right)\left(\frac{1-h\gamma}{1+h\gamma}\right) \tag{A19}$$

APPENDIX B. COMPUTER SIMULATIONS

We used numerical simulations to accompany and illustrate analytical results. We performed two types of simulations; one with fixed trait values and one where trait values evolved as an effect of mutations. Populations consisted of a discrete number of individuals. In order to obtain large population densities (C^* as above is typically less than one) we amplified consumer densities with a factor p by setting $C'_k = pC_k$ where C_k is the dimensionless measure. In the new units (indicated by [′]) the per capita growth rate at a given time step t is given by rescaling (the complete stochastic version of) eq. 6 and we obtain:

$$\begin{aligned} &w\left(z,\mathbf{C}'_t,\mathbf{z},\varepsilon_{1,t},\varepsilon_{2,t}\right)= \\ &1-d+a(z,Z_1)\left(e^{\varepsilon_{1,t}}-\sum_k a(z_k,Z_1)\frac{C'_{k,t}}{p}\right)+a(z,Z_2)\left(e^{\varepsilon_{k_t}}-\sum_k a(z_k,Z_2)\frac{C'_{k,t}}{p}\right) \end{aligned} \tag{B1}$$

At each time-step we calculated the expected individual fitness given by eq. (B1) which renders the expected population size according to:

$$E\left[C'_{k,t+1}\left|C'_{k,t},\varepsilon_{1,t},\varepsilon_{2,t}\right.\right]=C'_{k,t}\,w\left(z_k,\mathbf{C}'_t,\mathbf{z},\varepsilon_{1,t},\varepsilon_{2,t}\right),\ k=1,\ldots,n \tag{B2}$$

Demographic stochasticity was included by letting the actual population size be given as a Poisson distributed variable with the expected population size as parameter. In this way the model is equivalent to an individual based model, where each individual produces a Poisson distributed number of offspring.

For evolutionary simulations, mutant individuals were introduced with a probability m per offspring. The trait value z of the mutant was picked from a normal distribution with the trait value of the parent individual as mean and standard deviation σ_m. All mutant individual founded new populations, growing as described above. Correlation and autocorrelation of the environmental variables $\varepsilon_{1,t}$ and $\varepsilon_{2,t}$ were modelled according to eq. (10). Correlated random numbers were generated by multiplying a Cholesky decomposition of the covariance matrix with a vector of uncorrelated random numbers with zero mean and unit variance.

For all simulations $m = 5 \times 10^{-4}$, $\sigma_m = 0.002$, $d = 1.2$, $a_0 = 1.8$ and $\sigma_a = 0.8$. The factor p was set so that equilibrium densities were large, thereby ensuring that demographic stochasticity did not affect *CV* nor probability of branching (cf. Claessen et al 2007). More precisely, the population size of a single maximally specialized consumer using a single resource (e.g. corresponding to z = 1 and very small σ_a) was 100 000 individuals. With the parameters used, the expected population sizes for single consumers and two consumers with symmetrical z-values ranges always exceeds this number (using eq. A2 and A8). In simulations for measuring the *CV* (Figure 2 and 4A) σ_ε was chosen low so that no extinctions occurred whereas higher values were chosen for illustrating extinction risks (Figure 3 and 4B).

LITERATURE CITED

Abrams, P. A., H. Matsuda, and Y. Harada. 1993. Evolutionarily unstable fitness maxima and stable fitness minima of continuous traits. *Evolutionary Ecology* 7:465-487.

Box, G. E. P., and G. M. Jenkins. 1970, *Time series analysis: forecasting and control*. San Francisco, USA, Holden-Day.

Brown, J. S., and N. B. Pavlovic. 1992. Evolution in heterogeneous environments - effects of migration on habitat specialization. *Evolutionary Ecology* 6:360-382.

Caswell, H., and J. E. Cohen. 1995. Red, white and blue - environmental variance spectra and coexistence in metapopulations. *Journal of Theoretical Biology* 176:301-316.

Claessen, D., J. Andersson, L. Persson, and A. M. de Roos. 2007. Delayed evolutionary branching in small populations. *Evolutionary Ecology Research* 9:51-69.

Dercole, F. 2003. Remarks on branching-extinction evolutionary cycles. *Journal of Mathematical Biology* 47:569-580.

Dieckmann, U., and R. Law. 1996. The dynamical theory of coevolution: a derivation from stochastic ecological processes. *Journal of Mathematical Biology* 34:579-612.

Diekmann, O., P.-E. Jabin, S. Mischler, and B. Petrthame. 2005. The dynamics of adaptation: an illuminating example and a Hamilton-Jacobi approach. *Theoretical Population Biology* 67:257-271.

Doebeli, M., and U. Dieckmann. 2000. Evolutionary branching and sympatric speciation caused by different types of ecological interactions. *American Naturalist* 156:S77-S101.

Egas, M., U. Dieckmann, and M. W. Sabelis. 2004. Evolution restricts the coexistence of specialists and generalists: the role of trade off structure. *American Naturalist* 163:518-531.

Geritz, S. A. H., É. Kisdi, G. Meszéna, and J. A. J. Metz. 1998. Evolutionary singular strategies and the adaptive growth and branching of the evolutionary tree. E*volutionary Ecology* 12:35-57.

Gourbiere, S. 2004. How do natural and sexual selection contribute to sympatric speciation? *Journal of Evolutionary Biology* 17:1297-1309.

Gyllenberg, M., K. Parvinen, and U. Dieckmann. 2002. Evolutionary suicide and evolution of dispersal in structured metapopulations. *Journal of Mathematical Biology* 45:79-105.

Ito, H. C., and U. Dieckmann. 2007. A new mechanism for recurrent adaptive radiations. *American Naturalist* 170:E96-E111.

Iwasa, I., A. Pomiankowski, and S. Nee. 1991. The evolution of costly mate preferences. II. The handicap principle. *Evolution* 45:1431-1442.

Johansson, J., and J. Ripa. 2006. Will sympatric speciation fail due to stochastic competitive exclusion? *American Naturalist* 168:572-578.

Kisdi, É., F. J. A. Jacobs, and S. A. H. Geritz. 2001. Red Queen evolution by cycles of evolutionary branching and extinction. *Selection* 2:161-178.

Klemola, T., K. Norrdahl, and E. Korpimaki. 2000. Do delayed effects of overgrazing explain population cycles in voles? *Oikos* 90:509-516.

Lande, R. 1979. Quantitative genetic analysis of multivariate evolution, applied to brain:body size allometry. *Evolution* 33:402-416.

Lawton, J. H. 1988. More time means more variation. *Nature*:334:563.

MacArthur, R. H., and E. O. Wilson. 1967, *The theory of island biogeography*. Princeton, NJ, Princeton University Press.

Massin, N., and A. Gonzalez. 2006. Adaptive radiation in a fluctuating environment: disturbance affects the evolution of diversity in a bacterial microcosm. *Evolutionary Ecology Research* 8:471-481.

Matessi, C., A. Gimelfarb, and S. Gavrilets. 2001. Long-term build-up of reproductive isolation promoted by disruptive selection: How far does it go? . *Selection* 2.

Matsuda, H., and P. A. Abrams. 1994. Runaway evolution to self-extinction under asymmetrical competition. *Evolution* 48:1764-1772.

May, R. M. 1973. Stability in randomly fluctuating versus deterministic environments. *American Naturalist* 107:621-650.

Metz, J. A. J., S. A. H. Geritz, G. Meszena, F. J. A. Jacobs, and J. S. van Heerwaarden. 1996. Adaptive dynamics, a geometrical study of the consequences of nearly faithful reproduction., Pages 183-231 in S. J. Van Strien, and S. M. Verduyn Lunel, eds. *Stochastic and spatial structures of dynamical systems* Amsterdam, Elsevier.

Moran, P. A. P. 1953. The statistical analysis of the Canadian lynx cycle. II. Synchronization and meteorology. *Australian Journal of Zoology* 1:291-298.

Parvinen, K. 2005. Evolutionary suicide. *Acta Biotheoretica* 53:241-264.

Petchey, O. L., A. Gonzalez, and H. B. Wilson. 1997. Effects on population persistence: the interaction between environmental noise colour, intraspecific competition and space. *Proceedings of the Royal Society of London B, Biological Sciences* 264:1841-1847.

Pimm, S. L., and A. Redfearn. 1988. The variability of animal populations. *Nature* 334:613-614.

Polechova, J., and N. H. Barton. 2005. Speciation through competition: A critical review *Evolution* 59:1194-1210.

Ripa, J. 2009. When is sympatric speciation truly adaptive? An analysis of the joint evolution of resource utilization and assortative mating. *Evolutionary Ecolog*y 23(1): 31-52

Ripa, J. and Heino, M. 1999. Linear analysis solves two puzzles in population dynamics: the route to extinction and extinction in coloured environments. *Ecology Letters*, 2: 219-222.

Ripa, J., and A. R. Ives. 2003. Food web dynamics in correlated and autocorrelated environments. *Theoretical Population Biology* 64:369-384.

Ripa, J., and P. Lundberg. 1996. Noise colour and the risk of population extinctions. *Proceedings of the Royal Society Biological Sciences Series B* 263:1751-1753.

—. 2000. The route to extinction in variable environments. Oikos 90:89-96.

Ripa, J., P. Lundberg, and V. Kaitala. 1998. A general theory of environmental noise in ecological food webs. *American Naturalist* 151:256-263.

Roughgarden, J. 1975. Population dynamics in a stochastic environment: spectral theory for the linearized N-species Lotka-Volterra competition equations. *Theoretical Population Biology* 7:1-12.

Rueffler, C., T. J. M. Van Dooren, and J. A. J. Metz. 2006. The evolution of resource specialisation through frequency-dependent and frequency-independent mechanisms. *American Naturalist* 167:81-93.

Steele, J. H. 1985. A comparison of terrestrial and marine ecological systems. *Nature* 313:355-358.

Vincent, T. L., Y. Cohen, and J. S. Brown. 1993. Evolution via strategy dynamics. *Theoretical Population Biology* 44:149-176.

Waxman, D., and S. Gavrilets. 2005. Issues of terminology, gradient dynamics and the ease of sympatric speciation in Adaptive Dynamics. *Journal of Evolutionary Biology* 18:1214-1219.

FIGURE CAPTIONS

Figure 1. Ecological and evolutionary model. The trait value, z_j, of a single consumer species j gives its utilization of resource 1 and resource 2. More precisely, the attack rate $a(z)$ on each resource is read as the height of the Gaussian curve, centred at z_j, at $z = -1$ and $z = +1$, respectively. The niche width σ_a is represented by a double arrow. Equilibrium population sizes of two resource species, R_1^*, R_2^* are shown by black vertical bars situated at their corresponding z-values ±1. The difference in resource population size is a consequence of the consumer being more specialized on the resource at $z = 1$ compared to the resource at $z = -1$.

Figure 2. *CV* during evolutionary branching. CV for one (CV_I) and two (CV_{II}) consumer types is plotted as a function of the trait value z. In the two species case, only CV for the consumer type with $z > 0$ is shown. Analytic values are shown by dashed lines and values from simulations are shown by bold lines for one (grey) and two (black) consumer types. Simulations were done with 50 000 generations. The direction of monomorphic and dimorphic evolution are shown by arrows. Parameters: $\sigma_\varepsilon^2 = 0.005$, $\rho = 0$ and $\gamma = 0$.

Figure 3. Extinction risk during evolutionary branching. A. Extinction risk, measured as number of simulations (out of 100) where consumer populations went extinct before the maximal simulation time (50000 generations), for different values of z. Dashed line: single consumer extinction risk; Solid line: extinction risk for any of the two symmetric consumers. B and C. Comparison of the population dynamics of two generalists (B) and two specialists (C). Each point represents population sizes at given time-step and the ellipses enclose an estimated 95% of the points. The axis are normalised so that 1 corresponds to mean population density. The intensity of gray

indicates the risk of going extinct in the next time step for a given population density combination. The extinction risk was measured as the number of times out of 1000 trials where at least one of the populations got non-positive density in eq. 5. D. Repeated evolutionary branching. Each point represents a clonal population with a certain z-value. Parameters: (A,D) $\sigma_\varepsilon^2 = 0.015$, (B,C) $\sigma_\varepsilon^2 = 0.01$, $\rho = 0$ and $\gamma = 0$.

Figure 4. *CV*, extinction risk and simulations with highly autocorrelated fluctuations. A. *CV* for one and two species represented as in Figure 2. B. Extinction risk represented as in Figure 4A. C. Impeded branching due to autocorrelation. Parameters: $\rho = 0$, $\gamma = 0.95$, (A) $\sigma_\varepsilon^2 = 0.005$, (B,C) $\sigma_\varepsilon^2 = 0.015$.

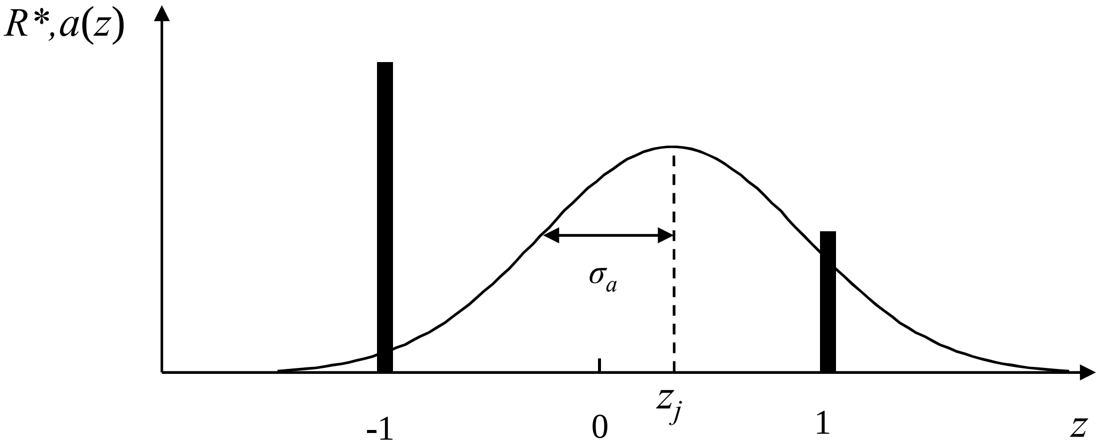

Figure 1.

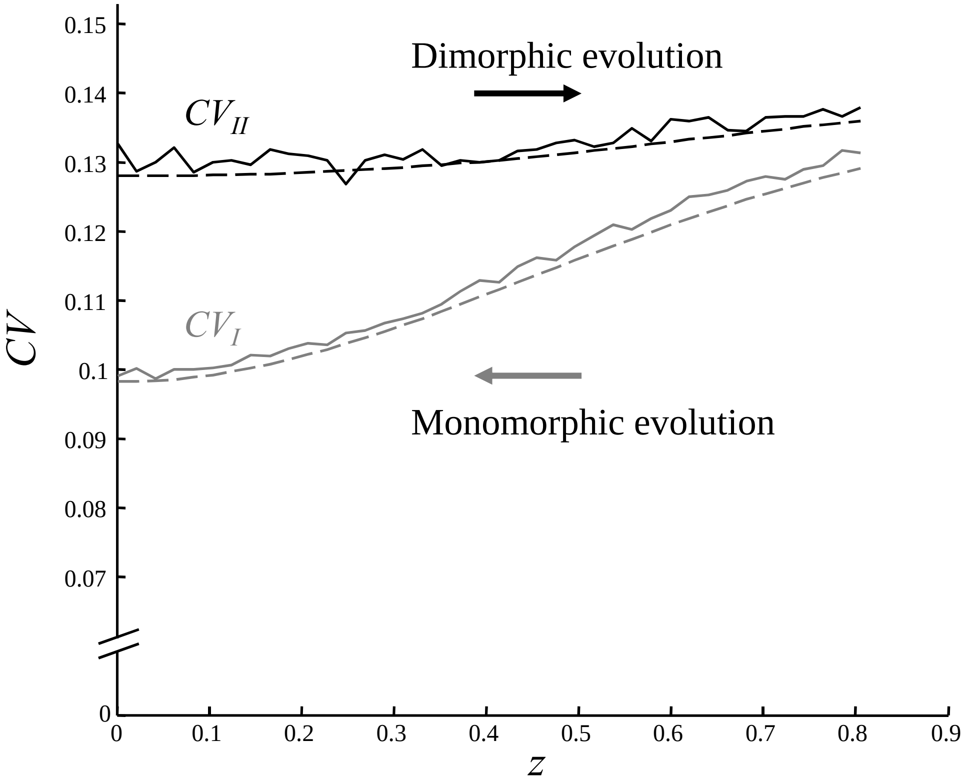
0.15
0.14
0.13
0.12
0.11
0.1
0.09
0.08
0.07
0
CV
0
0.1
0.2
0.3
0.4
0.5
0.6
0.7
0.8
0.9
z
Dimorphic evolution
CV_{II}
CV_I
Monomorphic evolution

Figure 2.

Figure 3.

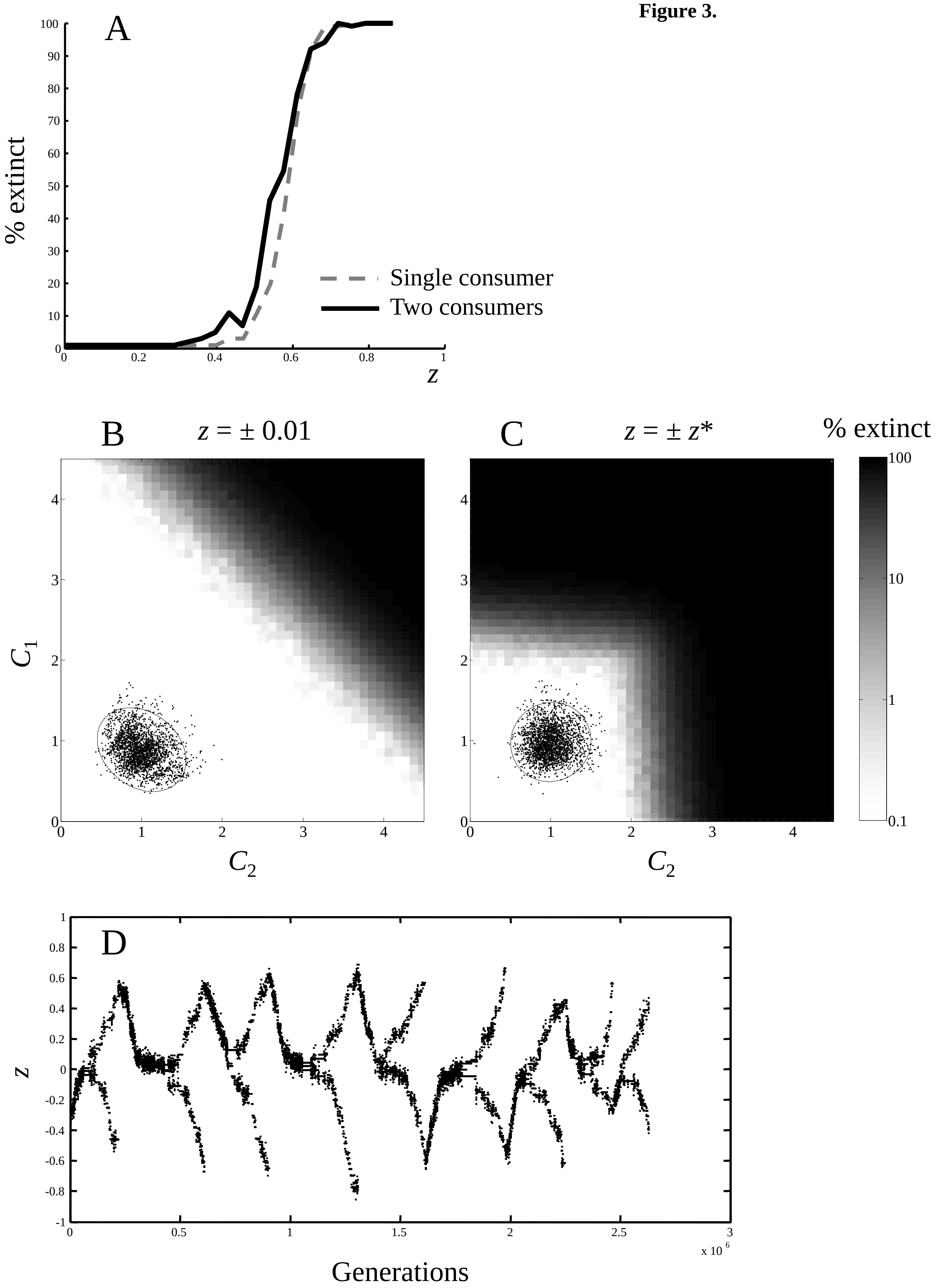
A
% extinct
100
90
80
70
60
50
40
30
20
10
0
0
0.2
0.4
0.6
0.8
1
z
Single consumer
Two consumers
B
z = ± 0.01
C
z = ± z*
% extinct
100
10
1
0.1
C1
C2
0
1
2
3
4
D
z
1
0.8
0.6
0.4
0.2
0
-0.2
-0.4
-0.6
-0.8
-1
0
0.5
1
1.5
2
2.5
3
x 10 6
Generations

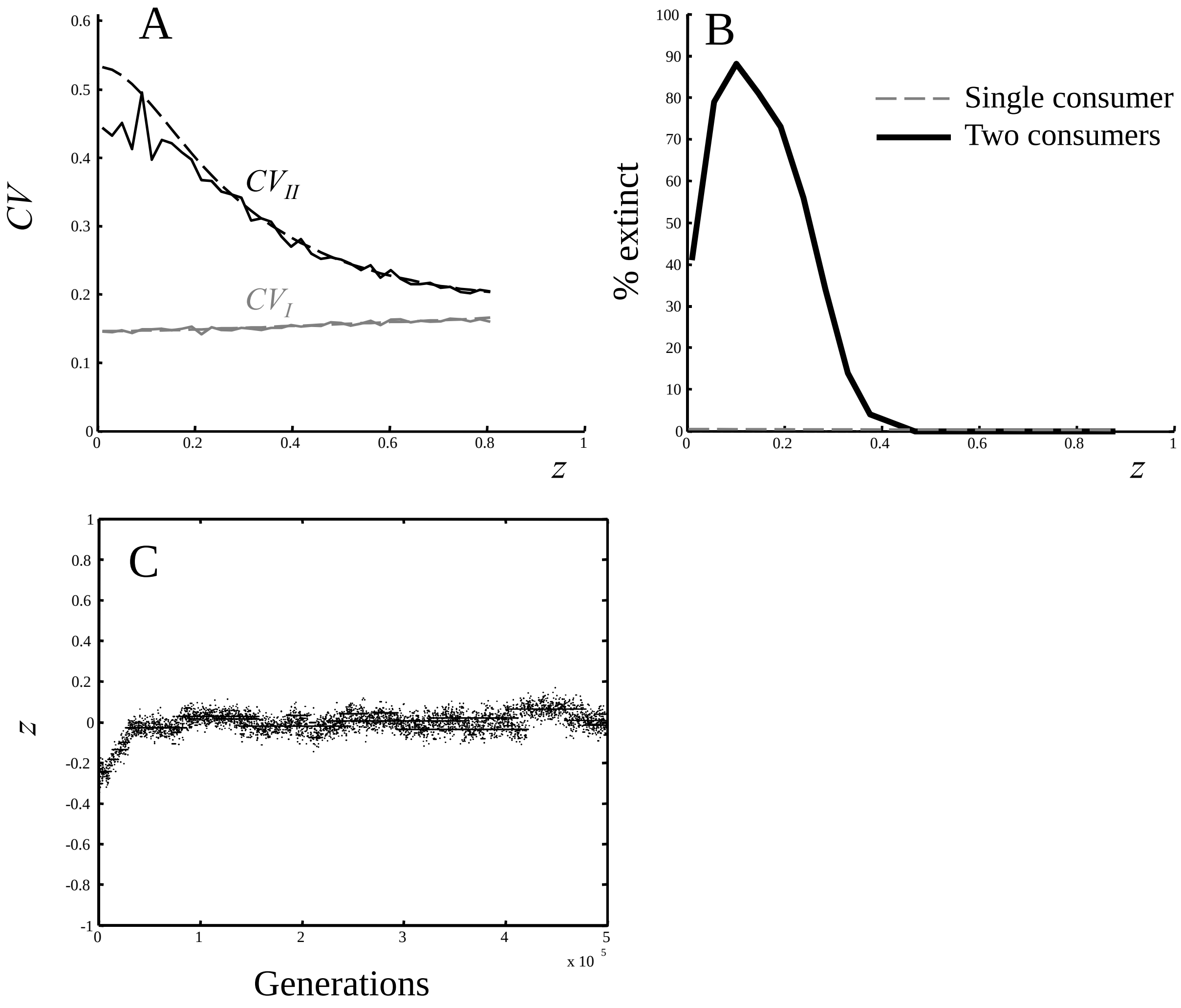
A
CV
CV_{II}
CV_I
0.6
0.5
0.4
0.3
0.2
0.1
0
0
0.2
0.4
0.6
0.8
1
z
B
% extinct
Single consumer
Two consumers
100
90
80
70
60
50
40
30
20
10
0
0
0.2
0.4
0.6
0.8
1
z
C
z
1
0.8
0.6
0.4
0.2
0
-0.2
-0.4
-0.6
-0.8
-1
0
1
2
3
4
5
x 10 5
Generations

Figure 4.